IEEE Access
Multidisciplinary | Rapid Review | Open Access Journal

Received December 31, 2018, accepted January 22, 2019, date of publication January 30, 2019, date of current version February 14, 2019.

Digital Object Identifier 10.1109/ACCESS.2019.2896356

A Conformal Magneto-Electric Dipole Antenna With Wide H-Plane and Band-Notch Radiation Characteristics for Sub-6-GHz 5G Base-Station

BOTAO FENG[1], (Member, IEEE), KWOK L. CHUNG[2], (Senior Member, IEEE), JIEXIN LAI[1], AND QINGSHENG ZENG[3], (Senior Member, IEEE)

[1]College of Electronic Science and Technology, Shenzhen University, Shenzhen 518060, China
[2]Civionics Research Laboratory, School of Civil Engineering, Qingdao University of Technology, Qingdao 266033, China
[3]College of Aeronautics, Nanjing University of Aeronautics and Astronautics, Nanjing 210016, China

Corresponding author: Kwok L. Chung (klchung@qut.edu.cn)

This work was supported in part by the International Cooperation Research Foundation of Shenzhen under Grant GJHZ20180418190621167, in part by the NTUT-SZU Joint Research Program under Grant 2018002, and in part by the State Key Laboratory of Metamaterial Electromagnetic Modulation Technology.

ABSTRACT This contribution presents a novel 3-D circular conformal MIMO antenna system composed of three magneto-electric dipoles (MED) antennas. The single MED element was delicately designed to include one main (lower-band) dipole and two auxiliaries (upper-band) dipoles in order to achieve the dual-band radiation. The proposed MED owns a low-profile conformal geometry but features a wide H-plane beamwidth (minimum 103°). By embedding the metamaterial of the broadside-coupled E-shaped unit cells into the magnetic dipole, the height of MED can be dramatically reduced by 37.2% as compared with the conventional ones. Meanwhile, the two U-shaped notches together with a rectangular notch were included onto the E-dipole to create a band-notch, which offers the anti-interference capability to the ubiquitous 2.4-GHz signal of the wireless local area network. According to the measurement results, the MED element exhibits an impedance bandwidth of 54.2% (1.68–2.93 GHz) with a stable gain of 6.05±1.15 dBi in the lower band and 9.2% (3.32–3.64 GHz) with 5.71 ± 0.7 dBi in the upper band, respectively. Moreover, the three-element MIMO system provides quasi-omnidirectional coverage in the H-plane from 1.68 to 3.64 GHz. The outstanding performance metrics validate the proposed ME dipole antenna that is well suited for the future sub-6-GHz fifth-generation MIMO mobile base stations.

INDEX TERMS Conformal antenna, magneto-electric dipole, miniaturization, MIMO antenna, 5G base-station antenna.

I. INTRODUCTION

With the increasing demand of high-speed data trans- mission and the coexistence of different kinds of communication networks, multi-frequency and wideband mobile communication systems have become a hot research area. In China, the frequency bands of 0.81-0.96 GHz and 1.71-2.69 GHz have been assigned to mobile networks for the 2G/3G/LTE communications [1]–[3]. Since November 2015, the 3.5 GHz C-band (3.4-3.6 GHz) has been distributed as the future mobile communication by the World Radio Communication Conference 2015 (WRC-15) [4]. As the 5G network offers massive users the ability to access with higher data rates, greater robustness and reduced power consumption, many research related to 5G wideband antennas were reported [5]–[7]. Due to the advantages such as enhancing channel capacity, improving the performances of transmitting and receiving signals, arranging massive antennas into a limited space and so on, the MIMO technology has become a core technology for 5G applications. Recently, several 5G MIMO antennas for smart phones were proposed [5]–[8]. By symmetrically placing two different antenna array types along the long edges of the system ground plane, a dual-polarized hybrid eight-antenna array operating in the 2.6-GHz band for 5G MIMO smartphone applications was proposed in [6]. Meanwhile, by using an 8×8 MIMO array instead of a single antenna, a hybrid antenna composed of two modules (4G and 5G antenna modules) was

The associate editor coordinating the review of this manuscript and approving it for publication was Ahmed Mohamed Ahmed Almradi.

proposed [7]. In [8], a 12-port massive MIMO antenna array was proposed for sub-6GHz mobile handset. However, literature on 5G MIMO base-stations antenna was rarely reported, owing to its design difficulty in such a wide frequency band. In China, integration of 2G/3G/LTE/5G communications by mainstream telecom operators have only used the frequency bands of 1.71-2.69 GHz and 3.3-3.6 GHz in order to fulfill the requirements of multi-network integration and save on upgrade costs.

In the past decade, owing to the outstanding radiation characteristics, such as the high unidirectional gain, low cross-polarization, high front-to-back ratio, as well as the possible wide H-plane radiation patterns, the unidirectional MED antenna, which was initiated by Luk and Wong [9], has been widely investigated and offered as a potential candidate for 5G communications [10], [11]. In [10], by employing a L-shaped feeding strip to excite a pair of dual-layer electric dipoles, a dual-band impedance bandwidth ranged from 0.78 GHz to 1.1 GHz and from 1.58 GHz to 2.62 GHz was achieved. With the dual-wideband bandwidth, this antenna can be used for 2G/3G/LTE application. In order to fulfill the requirements of wider bandwidth and enhance channel capacity, an antenna composing of five dual-polarized MED elements mounted on the five faces of a grounded metallic cubic structure was proposed for MIMO base-station application [11]. There, the four dual-polarized elements were rotationally combined in a ring-configuration, four different radiation patterns with polarization diversity were then achieved. However, both of these designs could not cover the 5G frequency band and were suffering from the bulky volume, which has been the major design challenge of MED antennas thus far. The conformal antenna array has advantages that include wide-angle coverage, space saving, and easy installation [12]–[14]. Therefore, arranging the antenna elements to form a miniaturized 3D conformal MIMO system is economical. The method can potentially solve the MED antenna's profile problem.

Nowadays the coexistence of many different kinds of ultrawideband and multi-frequency communication systems has been known as the design challenge for antenna engineers. This makes the anti-interference capability (AIC) an important performance indicator for high-performance antennas, especially in base-station applications. Various interesting antennas with band-notch characteristic for base-station and WLAN applications were proposed recently [15]–[17]. In order to reduce the number of antennas while expanding coverage to provide secure services for mobile users in dense environments, unidirectional antennas with high directivity and wide (H-plane) beamwidth become an urgent need. Research on the antennas with wide H-plane beamwidth were reported and achieved good performances [18]–[20]. Through introducing a modified trapezoid-shaped ground, the upper- and lower-frequency radiated dipoles were arranged with an inclined angle. Consequently, the beamwidth in the H-plane could vary over a range which was improved to 120° in the whole operating bandwidth in [18]. To increase the flexibility, by employing a feeding network with suitable element spacing and amplitude distribution cooperating with a three-element linear ME dipole array, a variable beamwidth could be obtained [19]. Nevertheless, their sizes proposed in [18]–[20] were still large and could not cover the 5G frequency band.

Recently, metamaterials have attracted much attention in physics and wireless communications communities because of the extraordinary electromagnetic characteristics, which have paved the way for the advancement of antenna design. These include polarization conversion, size miniaturization, gain enhancement, front-to-back radiation improvement of slot antennas, bandwidth broadening, so on and so forth [21]–[24]. In [21], by employing a 2D version of metamaterial known as metasurface with symmetrical window-shaped unit-cells, an antenna which converted linearly polarized (LP) signal to circularly polarized (CP) signal with wide return-loss bandwidth and high gain was proposed. Subsequently, by placing a thin metasurface on the top of CP slot antenna, the front-to-back radiation ratio was enhanced by 20 dB [22]. In [23], by arranging a metasurface composed of parallel strips on the top of a waveguide antenna, the linear polarization direction could rotate by 45°. In [24], by inserting a stack of split-ring resonators into a conventional MED antenna, the antenna height and volume could be reduced by 20% and 48%, respectively, as compared with the original antenna, without sacrificing antenna performance.

In this paper, a conformal metamaterial-embedded MED antenna and its 3D circular MIMO antenna system are presented. The triple-element MIMO antenna exhibits a quasi-omnidirectional radiation pattern with high directive gain in triple bands but occupies a smaller volumetric size. The following innovative techniques have been used in the design, which should be the contributions to the body of knowledge in the area of antenna design:

(i) Hi-&-Lo MED: three arc-shaped dipoles were delicately designed to create a dual-band in order to meet the frequency specifications of 2G/3G/4G-LTE/Sub-6GHz 5G;

(ii) Metamaterial embedding: a stack of metamaterials was embedded into the main MED, so that the antenna height is reduced by 37%;

(iii) Band-notch technique: two U-shaped slots together with a rectangular notch were included to afford the band-notch, which provides AIC to the ubiquitous 2.4 GHz WLAN signals; and,

(iv) Beamwidth enhancement and mutual coupling suppression technique: arc-shaped-cavity reflectors were conceived to achieve wide beamwidth and low mutual coupling for the 3D MIMO system.

The rest of this paper is organized as follows: Section II describes the geometries of the miniaturized Hi-&-Lo MED element as well as the 3-element 3D MIMO system. Section III delivers the innovative techniques stepwise addressing the design objectives, whereas the design simulation validated by the experimental results with a qualitative

comparison are presented in Section IV. Finally, conclusions are given in Section V.

II. DUAL-BAND CONFORMAL ANTENNA GEOMETRY

A. MINIATURIZED MED ANTENNA ELEMENT

The proposed antenna element consists of two types of arc-shaped MEDs having similar heights with respect to ground reflector after metamaterial embedding, a pair of arc-shaped fences as parts of cavity reflector, a stack of metamaterials composed of 14 layers of broadside-coupled E-shaped resonators arranged in double-sided 3×2 formats for the purpose of antenna height reduction. The Hi-&-Lo MED is composed of a main ME (lower-band) dipole and two auxiliary ME (upper-band) dipoles backed by a conformal reflector with a size of L1×L2, as illustrated in Fig. 1.

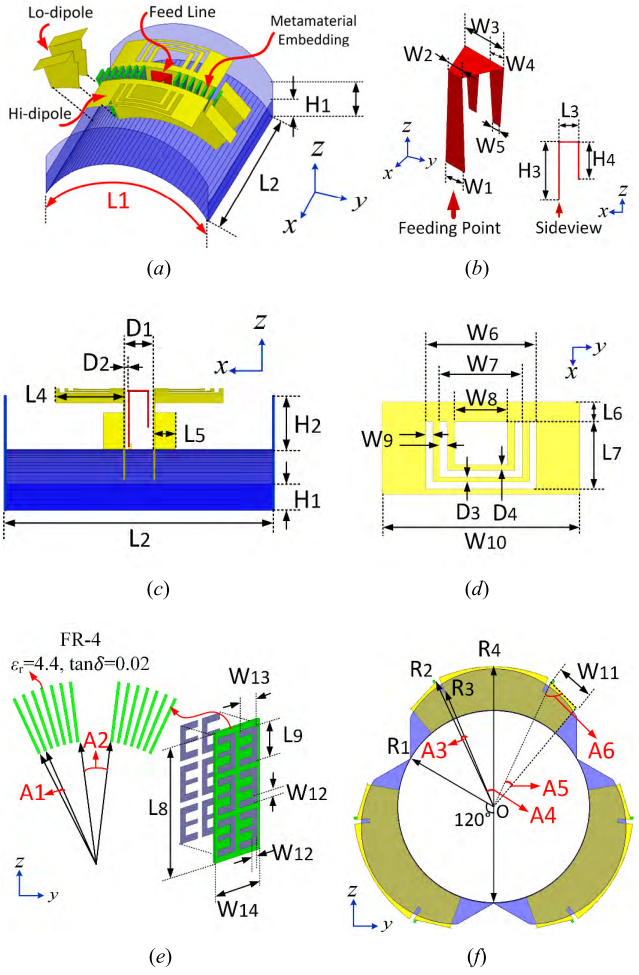

FIGURE 1. Geometry of the proposed antenna and its 3D MIMO system: (a) conformal Hi-&-Lo MED with metamaterial embedding, (b) folded-fork-shaped feed, (c) side-view of Hi-&-Lo MED, (d) slot-loading on Hi-dipole, (e) metamaterial composed of E-shaped unit-cells, (f) conformal three-element MIMO antenna system.

The arc-shaped, conformal structure subtends an angle of $2\pi/3$ that offers a wide H-plane radiation patterns, whereas the Hi-&-Lo MED provides dual-band impedance matching as well as dual-band radiation. A pair of U-shaped slots and a rectangular notch were consciously etched on the upper plane of the arc-shaped electric dipole (lower-band dipole). These notches cooperate with the metallic patch to generate a pair of currents in the opposite directions (see Fig. 4) to provide the band-notch radiation in the lower band. The arc-shaped fences (shorted-walls) together with the ground between them form a magnetic dipole. The electric dipole combined orthogonally with the magnetic dipole to constitute the ME dipole. The folded-fork-shaped feeding structure, composed of a vertical feed strip, a horizontal part and two coupling stubs, was employed to excite the main MED. Moreover, the broadside-coupled E-shaped resonators were designed and embedded into the main dipoles. As a result, the antenna height and the overall volume of MIMO antenna are significantly reduced.

B. CONFORMAL MIMO ANTENNA SYSTEM

Attributed to the wide H-plane feature of the conformal ME dipoles, a MIMO circular array composed of three dipole elements in a way that supports a quasi-360-deg coverage in H-plane was designed, as shown in Fig. 1(f). In order to improve the directivity of a single element and provide high isolation between elements, a conformal reflector was delicately designed with the addition of arc-shaped fences. The three elements were mounted evenly along the circumference of a circular ring having a radius of R1 to form a 3D conformal MIMO array. As a result, the mutual coupling between the MED elements can be effectively suppressed leading to excellent ECC performance, which is a key parameter of MIMO antenna system. Attributed to the inherent nature of the ME dipole and the distinct arc-shape design, the MIMO antenna system offers a stable gain performance, an omnidirectional coverage, a low ECC in a compact profile. The key geometrical parameters of the proposed ME dipole antenna and its 3-element MIMO system are summarized in Table 1.

TABLE 1. Geometrical parameters.

Parameter	L1	L2	L3	L4	L5	L6	L7
(mm)	96	95	7.8	25	10	4.6	19
Parameter	L8	L9	W1	W2	W3	W4	W5
(mm)	21	6	5	3.5	10.1	3.9	1.9
Parameter	W6	W7	W8	W9	W10	W11	W12
(mm)	30.5	23.2	15	2	53.6	18.3	1.1
Parameter	W13	W14	H1	H2	H3	H4	D1
(mm)	3.2	8	10	20	18.9	16.3	11.1
Parameter	D2	D3	D4	R1	R2	R3	R4
(mm)	1.3	1.5	1.5	45.9	65.9	59.7	67
Parameter	A1	A2	A3	A4	A5	A6	-
(degree)	3	14	1.7	22.9	15.5	67.7	-

III. TECHNIQUES ADDRESSING THE DESIGN GOALS

In order to fulfill the design specifications of the 5G mobile standards including the current standards (e.g. 3G and 4G-LTE), and the design objectives: a low-profile geometry yet wide beamwidth, high forward radiation, stable gain, smooth radiation patterns, low cross-polarization, and low mutual coupling, a number of innovative techniques were

applied to the design of the MIMO base-station system. The techniques addressing the design objectives are described in the following subsections. The key parameters in special structures were investigated by using ANSYS High Frequency Structure Simulation (HFSS) [25].

A. DUAL-BAND AND BAND-NOTCH TECHNIQUES

1) DUAL-BAND CONFORMAL MED

A dual band was created by using three conformal ME-dipoles with different sizes addressing the dual-band wide-beam requirements. The one with Hi-dipole (L4×W10) fulfills the lower-band requirement whereas the two (auxiliary) Lo-dipoles (L5×W11) address the upper-band operation. It should be noted that the Hi-Lo band performance is not just the impedance matching but also the gain suppression, as indicated in Fig. 2. The frequency band-gap (2.97-3.3 GHz) is created by the dual-band antenna, which are the unrelated frequencies of 2G/3G/LTE/5G.

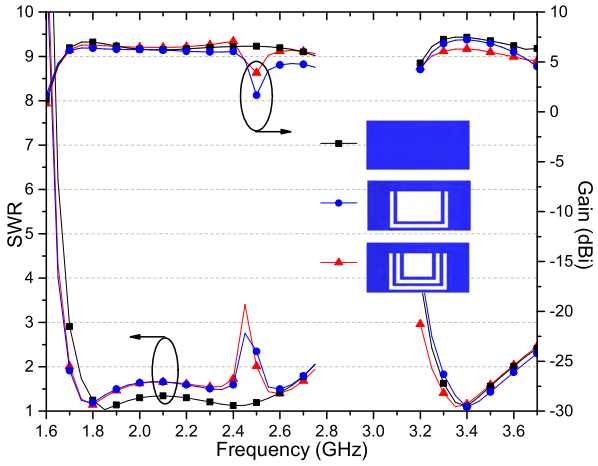

FIGURE 2. A comparison of band-notch performances when using combinations of different slots.

2) CREATION OF AIC/BAND-NOTCH AT 2.4 GHz

In addition to the dual-band operation, slot loading techniques were applied to the horizontal planes of the low-band dipole to address the need of anti-interference for the ubiquitous WiFi (2.4 GHz) signals. Fig. 2 shows the performance comparison for the design approach on different slot combinations. Without slots etched on the electric dipole, there is no band-notch around 2.4 GHz occurred on both SWR and gain curves. By using a window-shaped slot cooperating with a single U-slot, the band-notch on both the gain and SWR were created (blue curves), however, there was a gain drop below 5 dBi at the middle-band of 2.6-2.7 GHz. As a compromise, we chose the proposed slot combination, namely, use of two U-shaped slots and a window-shaped slot, in order to achieve stable gain across the frequency bands of interest. Fig. 2 shows the overall results of such design effort within the dual band, in particular, the broadside gain can be maintained above 5 dBi from the conformal design.

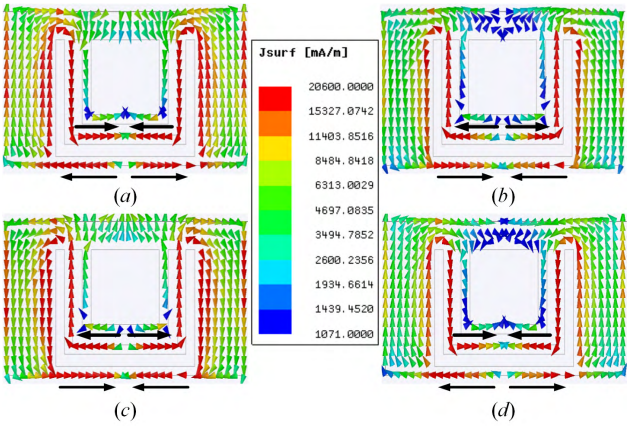

FIGURE 3. Current distributions at 2.40 GHz on the electric dipoles with slots loading in a period: (a) 0, (b) T/4, (c) T/2, and (d) 3T/4.

In order to showcase the effectiveness of the U-slots loading, the current distributions on the dipoles in a period of 2.4 GHz were examined, as displayed in Fig. 3. It is observed that the red currents are mainly distributed along the edges of U-shaped slots. In other words, the U-shaped notch patches play the primary radiating role at 2.4 GHz. At t=0, as shown in Fig. 3(a), the currents on the inner U-slot are flowing inward while the currents on the outer U-slot are flowing outward. The two-way currents flow in opposite directions and their effects will cancel out each other. As a result, the far-field radiation is eliminated to create the band-notch characteristic. At the time of T/4, the current directions shown in Fig. 3(b) are entirely opposed to that at t=0. This means that the main MED presents linearly polarization characteristics. Similarly, the current directions at the time of T/2 (Fig. 3(c)) are entirely opposed to that of 3T/4 (Fig. 3(d)). Noting that, the currents of the electric dipole become much stronger at t=0 than at t=T/4, whereas the currents on the magnetic dipole are opposed to the electric dipole. This reveals that the electric dipole and the magnetic dipole play a main radiating role in a cycle.

Through the fine-tune process using HFSS simulation, the horizontal length of U-shaped slots (W6), as shown in Fig. 1(d), was found to be a crucial parameter to produce the band-notch at 2.4 GHz, as well as the bandwidth in the lower band. As shown in Fig. 4, when W6 varies from 27.5 to 36.5 mm at an interval of 3 mm, the notch band around 2.4 GHz moves towards the lower frequencies and is getting wider. The effective lower frequency bands become narrow whereas the variation of bandwidth is limited in the upper band. In order to obtain the notch band (2.4-2.4825 GHz) and cover the lower-band (1.71-2.69 GHz), 30.5 mm was chosen as the optimal length of outer U-shaped slot (W6).

B. BEAMWIDTH ENHANCEMENT TECHNIQUE

In order to obtain the wide-beam (H-plane) pattern in the frequency bands of interest, especially for the Sub-6GHz 5G frequency bands, the dipoles were conceived as arc-shaped

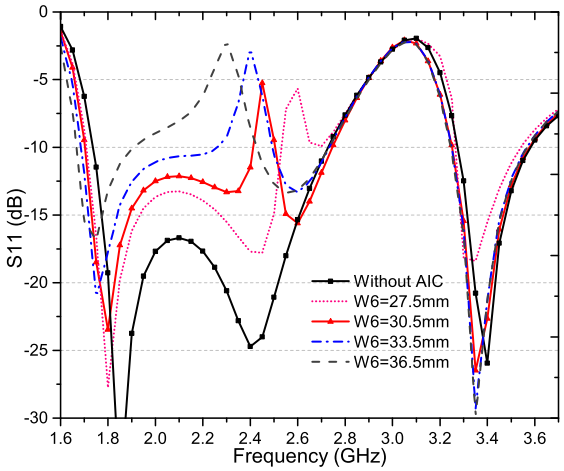

FIGURE 4. Effect of horizontal length of U-slots (W6) on the impedance matching of the dual-band MED.

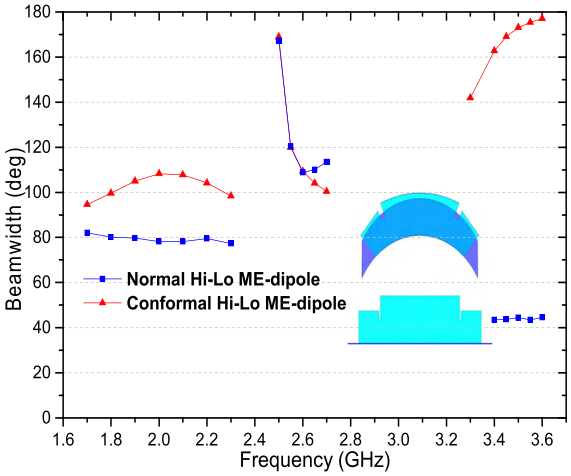

FIGURE 5. Comparison of half-power beamwidth performance (H-plane) on different types of Hi-&-Lo MED.

(conformal) structures with different heights, R4 and R2, respectively, with respect to the center of MIMO system (Fig. 1(f)). A comparison on the achievable half-power beamwidth (HPBW) between the ordinary planar-shape and arc-shape dipoles is shown in Fig. 5. With the proposed arc-shaped dipoles, HPBW of 102±7°, 135±34°, 160±15° were achieved for the bands ranged from 1.67 to 2.38 GHz, from 2.48 to 2.75 GHz, and from 3.3 to 3.6 GHz, respectively. It can be observed that by using the proposed conformal structure the HPBW is much wider than the ordinary one in the upper and lower frequency bands. Overall, the proposed structure can provide 20-30° beamwidth improvement in H-plane at the lower band, whereas over 120° beamwidth improvement for the Sub-6-GHz frequency band of 3.3-3.6 GHz. Under the ideal condition that all three MIMO elements are radiating simultaneously, Figs. 6(a)–(d) display the all radiation patterns at the essential frequencies within the upper and lower bands. As the HPBW of each element is sufficient wide, the composite (superposition) radiation patterns are virtually omnidirectional in H-plane. As a result, the proposed design

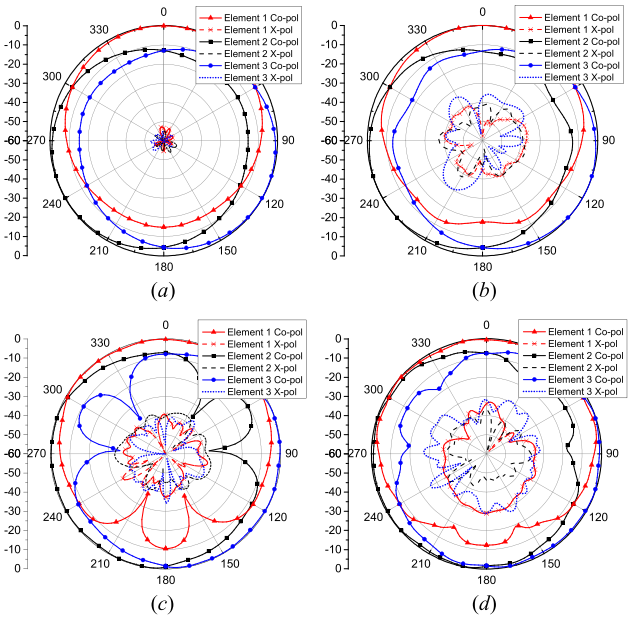

FIGURE 6. Simulated co-polarization patterns of three-element MIMO antenna system at (a) 1.7 GHz, (b) 2.6 GHz, (c) 3.3 GHz and (d) 3.5 GHz.

effectively reduces the required number of antenna elements for the 360° coverage. Nevertheless, the back-lobe variations at high frequencies are observed from Figs. 6(c) and 6(d).

C. MED MINIATURIZATION TECHNIQUE

Conventional MED antenna has the inherent disadvantage on its antenna profile in volumetric size, which makes it unattractive for modern base-station applications. Recently, a technique of metamaterial ($\varepsilon_r = 4.4$, $\mu_r = 1.8$) loading was proposed in [24], wherein the antenna operating frequency band is shifted to lower frequencies so that its height and volume of MED can be reduced by 20% and 48%, respectively. In this study, the authors carried forward another embedding technique for the Hi-dipole (lower-band) as shown in Fig. 1.

In this miniaturization process, broadside-coupled E-shaped resonators were designed (Fig. 1(e)) as meta-atoms printed on opposite sides of the 1-mm thin dielectric laminates of FR4 (μr=1, εr=4.4) for the fabrication of metamaterial. Fig. 7(a) shows the geometry of the unit-cell with dimensions. Conventional retrieval methods [26], [27] were studied to obtain the effective constitutive parameters of the embedded metamaterial. They are composed of two stacks of seven FR4 and airgap layers with a central gap, which is attributed to the occupation of the folded-fork-shaped feed structure. Plane wave illumination was applied onto the unit-cell along z-direction with an average periodicity of 2.95 mm along y-direction in order to obtain the transmission coefficient (S21) and reflection coefficient (S11), as shown in Figs. 7(b) and 7(c). Finally, a unique extraction procedure based on the Kramers-Kronig relationship [27] was used to compute the effective epsilon (ε_{eff}) and effective mu (μ_{eff}) as a function of frequency, as displayed in

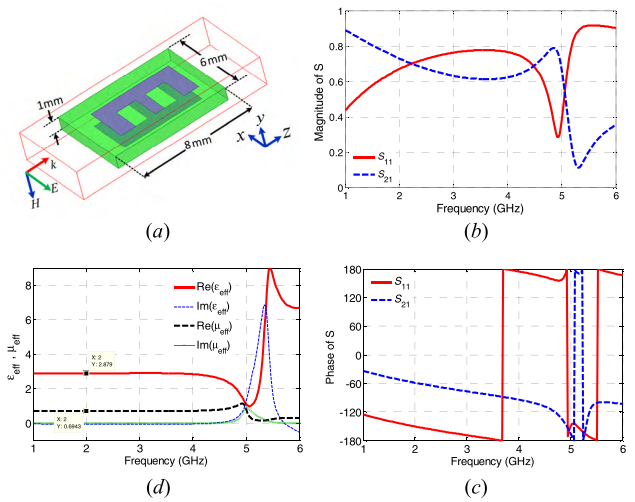

FIGURE 7. Effects on the S-parameters with different material embeddings.

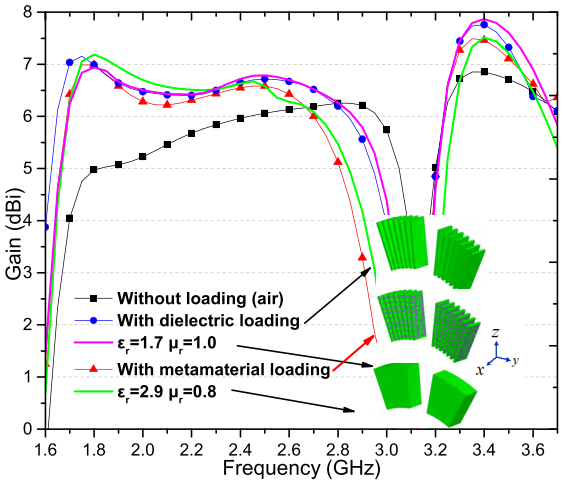

FIGURE 9. Effects on broadside gain of Hi-&-Lo MED with different material embeddings.

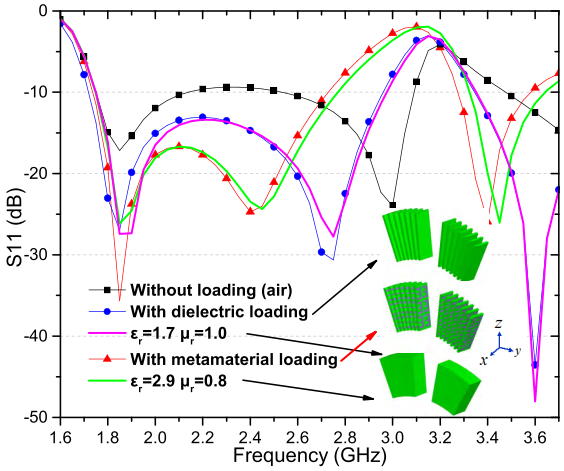

FIGURE 8. Effects on the S-parameters with different material embeddings.

Fig. 7(d). As expected, both the effective parameters are almost constant and recorded around 2.88 and 0.69, respectively, at the lower frequencies till 4 GHz. Although this is an approximated model for the real conformal metamaterial embedding, its results are found to be reasonable when compared to the results obtained from direct simulation. Fig. 8 shows the reflection coefficients (S11) of the Hi-&-Lo ME dipole after loading/embedding with different types of material, namely, air (no embedding), dielectric (layers of FR4 and airgap without meta-atoms), a lossless homogenous dielectric material ($\varepsilon_r = 1.7$ and $\mu_r = 1.0$), the proposed metamaterial (E-shaped resonators), and a lossless homogeneous magneto-dielectric material ($\varepsilon_r = 2.9$ and $\mu_r = 0.8$). It is observed that the proposed MED with the dielectric loading (blue curve) has a S11 performance that is close to the loading by a homogenous dielectric material (pink curve). Likewise, with metamaterial embedding (red curve) which is nearly the same as that with lossless homogeneous magneto-dielectric (green curve), the −10dB impedance bandwidth was recorded from 1.74 to 2.73 GHz. Similar observation is established for the broadside (realized) gain performance with different types of material embedding, as shown in Fig. 9. The antenna with metamaterial loading exhibits less gain fluctuation in the broadside than that of MED with dielectric loading. The small gain difference between the green and red curves is attributed to the finite dielectric loss from the FR4 laminates. That is to say, by placing the dielectric material (without the E-shaped resonators) along the magnetic field, the effective epsilon can be reduced to 1.7 within the working bandwidths. However, by place the proposed metamaterial inside the MED, the ε_{eff} is increased to 2.9 while μ_{eff} is reduced to 0.8.

D. MUTUAL COUPLING AND BACKWARD RADIATION SUPPRESSION TECHNIQUE

A folded trapezoid-shaped ground plane was firstly proposed in [18] for enhancement of beamwidth and front-to-back ratio (FBR) of ME-dipole. In this design, a conformal cavity ground plane (reflector), denoted as arc-shaped cavity reflector, was delicately devised in order to meet the specifications of high isolation and FBR for the 5G base-station antenna, as shown in Fig. 1(a). The technique includes the addition of arc-shaped fences at the H-plane (denoted as H-plane fences) with an arc-length (L1) of 96 mm and a height (H2) of 20 mm to form a conformal cavity. This technique not only suppresses the mutual coupling and the backward radiation, but also enhances the H-plane beamwidth. Fig. 10 shows the performances with the addition of H-plane fences as compared with arc-shaped reflector only. As shown, the FBR was improved as high as by 3.3 dB and 15 dB in the upper and lower frequency band, respectively. Moreover, with the addition of H-plane fences, the beamwidth is able to expand by 49° and 38° maximum in the upper and lower band, respectively.

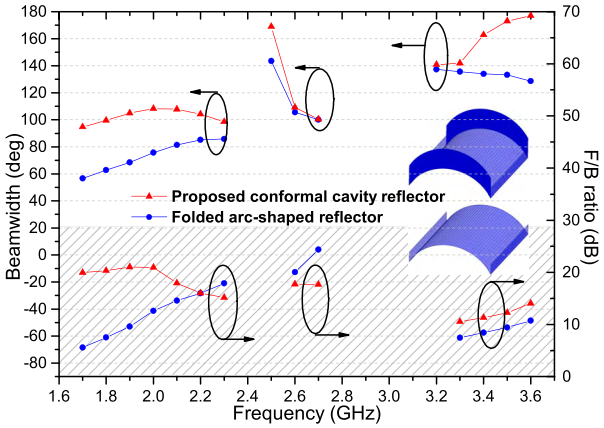

FIGURE 10. Beamwidth and F/B ratio enhancement after including fences.

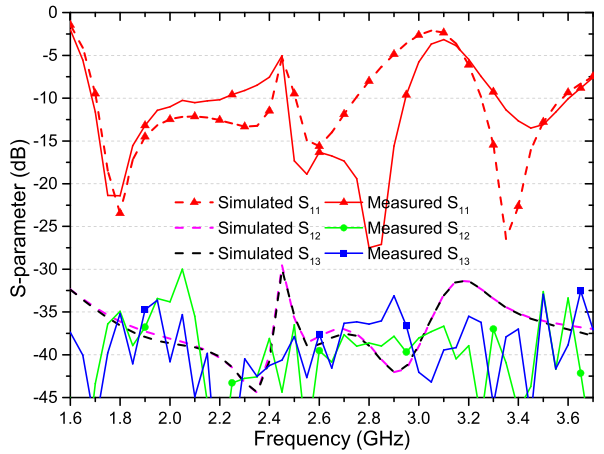

FIGURE 11. Reflection coefficient and mutual coupling of the proposed three-element MIMO antenna system.

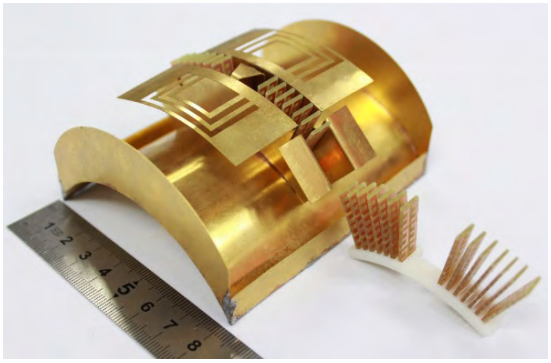

(*a*)

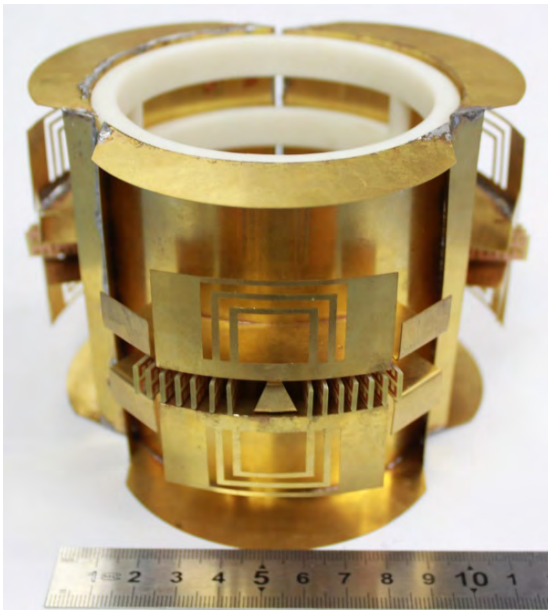

(*b*)

FIGURE 12. Photographs of (a) the proposed Hi-&-Lo MED element with metamaterial embedding, and (b) the 3D-MIMO system composed of triple ME-dipoles.

Figure 11 shows the mutual coupling between elements, S12 and S13, as well as the reflection coefficient S11 within the bands. As seen, the mutual coupling are all below -30 dB and with a small fluctuation in the entire frequency band, except the AIC at 2.4 GHz. It indicates that the arc-shaped-cavity reflector cooperates with the separated arc-shaped electric dipole to obtain not only stable FBR but also wide 3-dB beamwidth as well as good isolation (low mutual coupling) among the MED elements.

IV. VALIDATION AND DISCUSSION

To validate the proposed conformal design, prototypes of a single Hi-&-Lo MED element and its three-element MIMO system were fabricated and functionally tested. The corresponding photographs for the miniaturized prototypes are depicted in Figs. 12(a) and 12(b), respectively. The angular dimensions of the single MED element are $96\times95\times21.1$ mm^3. The measured results of the impedance matching in term of SWR, broadside gain, ECC and radiation patterns were attained by using the Agilent E5071C network analyzer and SATIMO antenna measurement system. These key performance metrics of the single MED antenna and the MIMO system are compared with the predicted results obtained from HFSS simulation.

The simulated impedance bandwidths of the single Hi-&-Lo MED element ranges from 1.70 to 2.75 GHz and 3.25 to 3.6 GHz (SWR $\leq$ 2) for lower and upper frequency bands, respectively, as shown in Fig. 13. A notch-band was created for the purpose of AIC in the lower band from 2.4 to 2.5 GHz. Correspondingly, the measured impedance bandwidth ranges from 1.68 to 2.93 GHz with a notch-band from 2.25 to 2.47 GHz, and 3.32 to 3.64 GHz (SWR $\leq$ 2) for the lower and upper frequency bands, respectively. These achieved dual wideband cover the Sub-6-GHz frequency bands used in China (namely, 1.71 GHz-2.69 GHz, 3.3 GHz-3.6 GHz), and with the AIC against the ubiquitous WiFi signals. The simulated gain varies between 5.6 dBi and 7.4 dBi in the lower band, and between 5.6 dBi and 6.1 dBi in the upper band, respectively. In comparison, the measured one

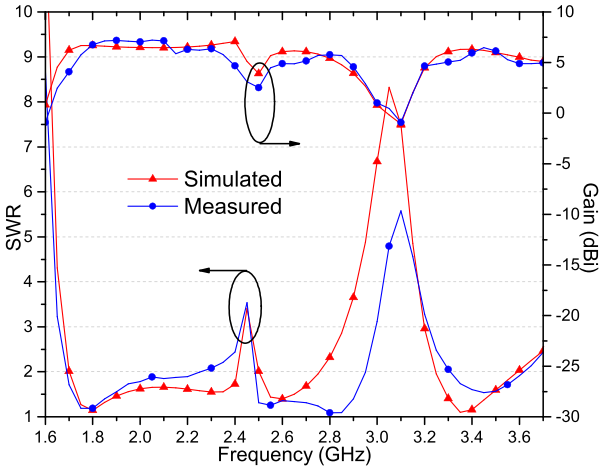

FIGURE 13. Simulated and measured SWR and gain of a single MED.

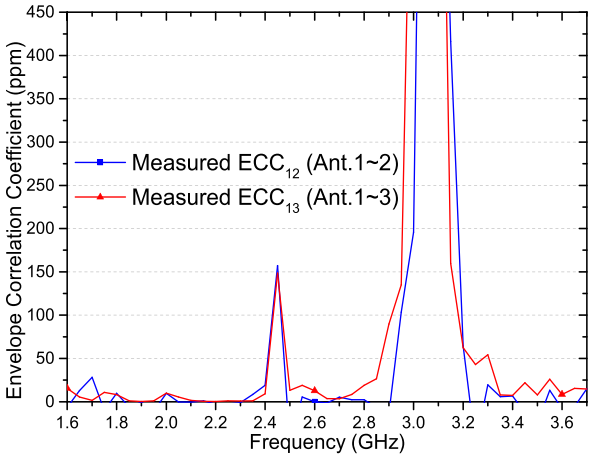

FIGURE 14. Measured ECC performance of the 3-element MIMO antenna system.

varies between 4.9 dBi and 7.2 dBi (namely, 6.05±1.15 dBi) in the lower band, and 5.75 ±0.75 dBi in the upper band, respectively. The measured results agree well with the simulated ones. It can be concluded that the gains are relatively stable and high enough for the 2G/3G/LTE/5G requirements.

In MIMO antenna systems, the system performance and antenna diversity can be quantified by using the envelope correlation coefficient (ECC) values between antenna elements [28], [29]. Small fading of the received signals demands a low ECC from a planar MIMO system. It was recommended that ECC should be less than 0.7 for a MIMO base-station and lower than 0.5 for a mobile handset [28]. To evaluate the diversity performance of the proposed three-element MIMO system, the crucial parameters such as the ECC (ρ_{eij}) and the mean effective gain (*MEG*) ratio are studied. They can be described by [28], [29]:

$$\rho_{eij} = [|\rho_{ij}| + \sqrt{(\frac{1}{\eta^i_{rad}} - 1)(\frac{1}{\eta^j_{rad}} - 1)}]^2 \quad (1)$$

$$\rho_{ij} = \frac{-S^*_{ii}S_{ij} - S^*_{ji}S_{ij}}{\sqrt{(1-(|S_{ii}|^2+|S_{ji}|^2))(1-(|S_{jj}|^2+|S_{ij}|^2))\eta^i_{rad}\eta^j_{rad}}} \quad (2)$$

$$MEG_i = \frac{\eta^i_{mis} \cdot \eta^i_{rad}}{2} = \frac{(1 - \sum_{j=1}^{N} |S_{ij}|^2) \cdot \eta^i_{rad}}{2} \quad (3)$$

$$\frac{MEG_i}{MEG_j} \cong 1 \quad (4)$$

where η_{rad} and η_{mis} represent the antenna radiation efficiency and the antenna mismatch efficiency, respectively. The subscripts, i and j, denote the ith and jth antenna elements, respectively. In this three-element MIMO system, $i = 1$ and $j = 2, 3$, whereas N is the total number of antenna elements.

In the proposed 3D conformal MIMO system, the mutual coupling between conformal MEDs were well suppressed by using the aforementioned techniques. The simulated ECCs of the MIMO antenna system, verified with measurement, are found to be far less than 100 ppm within the working bandwidths, as shown in Fig. 14. Moreover, the MEGs of all elements are almost identical attributed to high isolation, or low mutual coupling of less than −30 dB. Therefore, we conclude that the diversity performance of the proposed MIMO system is excellent.

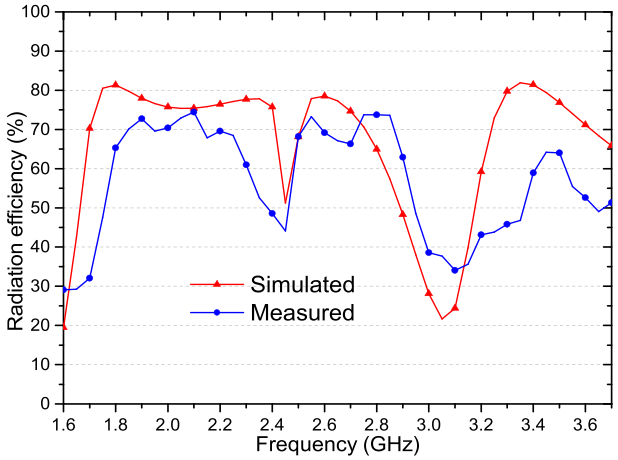

FIGURE 15. Measured radiation efficiency validates the simulated one.

Figure 15 shows a comparison on simulated and measured radiation efficiency of the Hi-&-Lo MED element, where good mutual agreement was obtained excepting at the high band. This could be attributed to the under-estimation of dielectric (FR4) loss at high frequencies in simulation. Fig. 16 displays the simulated and measured radiation patterns at the essential frequencies. In general, the measured results (right column) concurred with the predicted ones from simulation (left column) except small discrepancies attributed to fabrication and measurement tolerances. Symmetric unidirectional radiation patterns in the E- and H-planes over the operating bandwidths were obtained. At the lower band (1.71-2.69 GHz), the H-plane beamwidth and E-plane beamwidth are almost the same. However, at the upper band

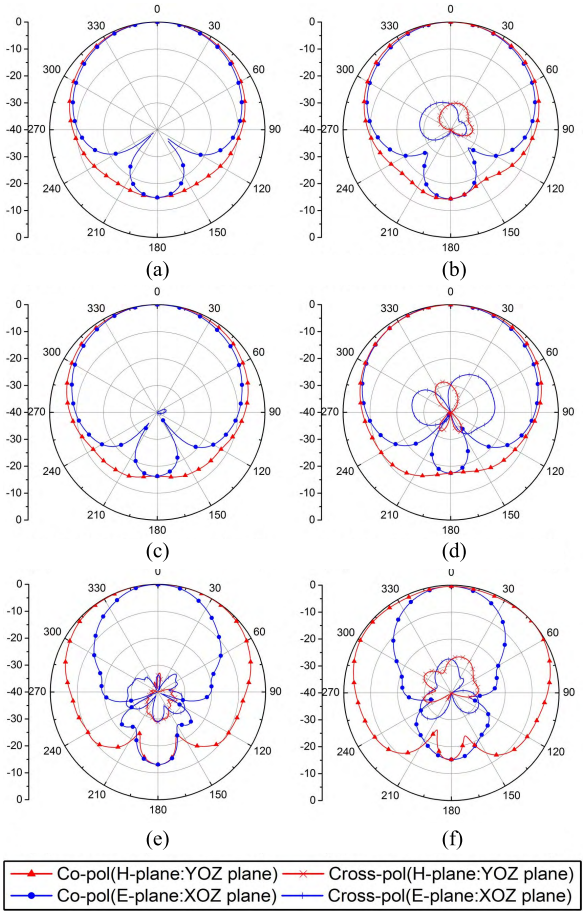

FIGURE 16. Measured radiation patterns confirmed to simulated ones in E- and H-plane at (a) 1.8 GHz, (b) 2.6 GHz and (c) 3.5 GHz.

TABLE 2. Size and performance comparison of single MED.

Refs.	ZBW (GHz)	HPBW (deg)	Gain (dBi)	ECC (<)	Element size (λ_0^3)
[10]	0.78-1.1 1.58-2.62	103±5 45±11	6.5±0.5 8.5±0.5	N.A.	0.69×0.69 ×0.179
[11]	1.77-2.62	N.A.	1.3±0.5	0.001	0.81×0.81 ×0.23
[15]	2.32-2.54 5-5.85	120±10	5±0.3	N.A.	1.21×1.21 ×0.48
[16]	1.83-2.92 2.39-2.52(BN)	N.A.	7.0±1.0	0.01	0.95×0.95 ×0.24
[17]	1.68-2.68 2.27-2.53(BN)	60±5	7.4±0.6	N.A.	1.10×1.10 ×0.24
[18]	2.37-3.76	118±5	6.7±0.4	N.A.	1.00×1.00 ×0.30
[19]	1.8-2.1	72±2	6.7±0.4	N.A.	1.58×1.14 ×0.25
[24]	1.70-2.67	77.8	8.2±0.3	N.A.	1.10×1.10 ×0.196
This work	1.68-2.93 2.25-2.47 (BN) 3.32-3.64	103±9 165±5	6.05±1.15 5.75±0.75	100 ppm	0.71×0.70 ×0.156

where λ_0 and BN represent the free-space wavelength at the mid-band frequency of lower band and band notch, respectively.

(3.3-3.6 GHz), the H-plane beamwidth is obtained much wider than that from the E-plane. This mainly attributed to (i) the conformal Hi-&-Lo MED design, and (ii) the corresponding arc-shaped cavity reflector. The measured H-plane beamwidth at 1.8 GHz, 2.6 GHz and 3.5 GHz are recorded as 103°, 116° and 168°, respectively. Meanwhile, the cross-polarization levels in E- and H-plane are generally below −22 dB by measurement whereas the FBRs are higher than 15 dB and 11 dB at the lower and upper band, respectively, from the measurement.

Table 2 shows a comparison between the proposed antenna and the reference base-station antennas in terms of operating bands (ZBW), HPBW, broadside gain, ECC and antenna volume. It can be observed that the proposed antenna owns the widest bandwidth with band-notch (AIC) function, the widest HPBW, the lowest ECC, smallest size and stable gain. The gain is slightly lower than some reference antennas due to its wide H-plane beamwidth. In summary, the MIMO system exhibits superior radiation characteristics, wide beam-widths, as well as excellent diversity performance.

V. CONCLUSIONS

A low-profile conformal ME dipole antenna with wide H-plane beamwidth and band-notch radiation characteristics is described in this paper. The electric dipoles are designed to have two separated arc-shaped planes with different heights and designated as the Hi-&-Lo MED in order to provide dual band and wide beamwidth characteristics. By embedding the broadside-coupled E-shaped resonators of metamaterial into the conformal magnetic dipole, the height of the MED significantly reduced by 37.2%. As a result, the volume of this single Hi-&-Lo MED and the volume of the three-element MIMO antenna can be reduced by about 30%, respectively. Indeed, with the anti-interference capability (band-notch) at 2.4 GHz, the proposed MED becomes a triple-band antenna with operating frequency bands of 1.68-2.25 GHz, 2.47-2.93 GHz and 3.32-3.64 GHz. In addition, the low envelope correlation coefficient, diversity performance and near omni-directional coverage are realized, making the proposed small ME dipole antenna an excellent candidate for the Sub-6-GHz 5G applications.

REFERENCES

[1] Y. Cui, R. Li, and P. Wang, "Novel dual-broadband planar antenna and its array for 2G/3G/LTE base stations," *IEEE Trans. Antennas Propag.*, vol. 61, no. 3, pp. 1132–1139, Mar. 2013.

[2] X.-W. Dai, Z.-Y. Wang, C.-H. Liang, X. Chen, and L.-T. Wang, "Multiband and dual-polarized omnidirectional antenna for 2G/3G/LTE application," *IEEE Antennas Wireless Propag. Lett.*, vol. 12, pp. 1492–1495, 2013.

[3] Z. Wang, X. Liu, Y. Yin, and J. Wu, "Dual-element folded dipole design for broadband multilayered Yagi antenna for 2G/3G/LTE applications," *Electron. Lett.*, vol. 50, no. 4, pp. 242–244, Feb. 2014.

[4] *World Radiocommunication Conference Allocates Spectrum for Future Innovation*. Accessed: Nov. 27, 2015. [Online]. Available: http://www.itu.int/net/pressofce/press_releases/2015/56.asp

[5] Y.-L. Ban, Z.-X. Chen, Z. Chen, K. Kang, and J. L.-W. Li, "Decoupled closely spaced heptaband antenna array for WWAN/LTE smartphone applications," *IEEE Antennas Wireless Propag. Lett.*, vol. 13, pp. 31–34, 2014.

[6] M.-Y. Li *et al.*, "Eight-port orthogonally dual-polarized antenna array for 5G smartphone applications," *IEEE Trans. Antennas Propag.*, vol. 64, no. 9, pp. 3820–3830, Sep. 2016.

[7] Y.-L. Ban, C. Li, C.-Y.-D. Sim, G. Wu, and K.-L. Wong, "4G/5G multiple antennas for future multi-mode smartphone applications," *IEEE Access*, vol. 4, pp. 2981–2988, 2016.
[8] Y. Li, C.-Y.-D. Sim, Y. Luo, and G. Yang, "12-port 5G massive MIMO antenna array in sub-6GHz mobile handset for LTE bands 42/43/46 applications," *IEEE Access*, vol. 6, pp. 344–354, 2018.
[9] K.-M. Luk and H. Wong, "A new wideband unidirectional antenna element," *Int. J. Microw. Opt. Technol.*, vol. 1, no. 1, pp. 35–44, Jun. 2006.
[10] W. X. An, H. Wong, K. L. Lau, S. F. Li, and Q. Xue, "Design of broadband dual-band dipole for base station antenna," *IEEE Trans. Antennas Propag.*, vol. 60, no. 3, pp. 1592–1595, Mar. 2012.
[11] S. Chen and K.-M. Luk, "A dual-mode wideband MIMO cube antenna with magneto-electric dipoles," *IEEE Trans. Antennas Propag.*, vol. 62, no. 12, pp. 5951–5959, Dec. 2014.
[12] X. Lan, L. Wang, Y. Wang, C. Choi, and D. Choi, "Tensor 2-D DOA estimation for a cylindrical conformal antenna array in a massive MIMO system under unknown mutual coupling," *IEEE Access*, vol. 6, pp. 7864–7871, 2018.
[13] P. Sanchez-Olivares, P. P. Sanchez-Dancausa, and J. L. Masa-Campos, "Circularly conformal patch array antenna with omnidirectional or electronically switched directive beam," *IET Microw., Antennas Propag.*, vol. 11, no. 15, pp. 2253–2259, Oct. 2017.
[14] S. Mohammadi, A. Ghani, and S. H. Sedighy, "Direction-of-arrival estimation in conformal microstrip patch array antenna," *IEEE Trans. Antennas Propag.*, vol. 66, no. 1, pp. 511–515, Jan. 2018.
[15] W. C. Zheng, L. Zhang, Q. X. Li, and Y. Leng, "Dual-band dual-polarized compact bowtie antenna array for anti-interference MIMO WLAN," *IEEE Trans. Antennas Propag.*, vol. 62, no. 1, pp. 237–246, Jan. 2014.
[16] H. Zhai, J. Zhang, Y. Zang, Q. Gao, and C. Liang, "An LTE base-station magnetoelectric dipole antenna with anti-interference characteristics and its MIMO system application," *IEEE Antennas Wireless Propag. Lett.*, vol. 14, pp. 906–909, 2015.
[17] H. Huang, Y. Liu, and S. Gong, "A broadband dual-polarized base station antenna with anti-interference capability," *IEEE Antennas Propag. Lett.*, vol. 16, pp. 613–616, 2017.
[18] Y. Li and K.-M. Luk, "A linearly polarized magnetoelectric dipole with wide h-plane beamwidth," *IEEE Trans. Antennas Propag.*, vol. 62, no. 4, pp. 1830–1836, Apr. 2014.
[19] L. Ge and K. M. Luk, "A three-element linear magneto-electric dipole array with beamwidth reconfiguration," *IEEE Antennas Wireless Propag. Lett.*, vol. 14, pp. 28–31, 2015.
[20] G. Idayachandran and R. Nakkeeran, "Unidirectional magneto-electric dipole antenna for base station: A review," *J. Inst. Eng. (India), B*, vol. 99, no. 2, pp. 211–220, 2018, doi: 10.1007/s40031-017-0313-5.
[21] H. L. Zhu, S. W. Cheung, K. L. Chung, and T. I. Yuk, "Linear-to-circular polarization conversion using metasurface," *IEEE Trans. Antennas Propag.*, vol. 61, no. 9, pp. 4615–4623, Sep. 2013.
[22] K. L. Chung and S. Kharkovsky, "Metasurface-loaded circularly-polarised slot antenna with high front-to-back ratio," *IET Electron. Lett.*, vol. 49, no. 16, pp. 979–981, Aug. 2013.
[23] H. L. Zhu, K. L. Chung, C. Ding, G. Wei, C. Zhang, and Y. J. Guo, "Polarization-rotated waveguide antennas for base-station applications," *IEEE Antennas Wireless Propag. Lett.*, vol. 16, pp. 1545–1548, 2017, doi: 10.1109/LAWP.2017.2648858.
[24] L. Mingjian, K.-M. Luk, K. Zhang, and L. Ge, "Miniaturization of magnetoelectric dipole antenna by using metamaterial loading," *IEEE Trans. Antennas Propag.*, vol. 64, no. 11, pp. 4914–4918, Nov. 2016.
[25] *ANSYS HFSS, Version 14*, ANSYS, Canonsburg, PA, USA, 2012.
[26] X. Chen, T. M. Grzegorczyk, B.-I. Wu, J. Pacheco, Jr., and J. A. Kong, "Robust method to retrieve the constitutive effective parameters of metamaterials," *Phys. Rev. E, Covering Stat., Nonlinear, Biol., Soft Matter Phys.*, vol. 70, no. 1, Feb. 2004, Art. no. 016608.
[27] Z. Szabo, G.-H. Park, R. Hedge, and E.-P. Li, "A unique extraction of metamaterial parameters based on Kramers-Kronig relationship," *IEEE Trans. Microw. Theory Techn.*, vol. 58, no. 10, pp. 2646–2653, Oct. 2010.
[28] R. G. Vaughan and J. B. Andersen, "Antenna diversity in mobile communications," *IEEE Trans. Veh. Technol.*, vol. VT-36, no. 4, pp. 147–172, Nov. 1987.
[29] S. C. Ko and R. D. Murch, "Compact integrated diversity antenna for wireless communications," *IEEE Trans. Antennas Propag.*, vol. 49, no. 6, pp. 954–960, Jun. 2001.

BOTAO FENG (M'14) received the B.S. and M.S. degrees in communication engineering from the Chongqing University of Posts and Telecommunications, Chongqing, China, in 2004 and 2009, respectively, and the Ph.D. degree in communication and information system from the Beijing University of Posts and Telecommunications, Beijing, China, in 2015. In 2004, he joined the Dongguan Branch, Nokia Mobile Phones, Ltd., China, as a Senior Communication Engineer. From 2009 to 2012, he was a Senior Research Fellow in mobile network optimization with China United Network Communications Company, Ltd. He is currently a Postgraduate Advisor and a Postdoctoral Advisor with Shenzhen University, Guangdong, China. He is also the Head of the Laboratory of Wireless Communication, Antennas, and Propagation, Shenzhen University, and the Director of Shenzhen Taobida Technologies, Co., Ltd. He and his team members are currently conducting over 10 projects on antenna development and design for 5G/THz and future communications, which are supported by the natural science research funds and the industrial cooperation research and development funds. He has authored more than 30 SCI- and EI-indexed papers. He holds over 20 invention patents. His research interests include base-station antenna, microcell antenna, indoor antenna, and wireless network optimization. He serves as a Peer Reviewer and a Technical Committee Member of IEEE/IET, Elsevier, Wiley, and Springer journals and conferences on microwave technique and antenna.

KWOK L. CHUNG (S'00–M'05–SM'11) received the B.E. (Hons.) and Ph.D. degrees in electrical engineering from the University of Technology Sydney, Australia, in 1999 and 2005, respectively. In 2004, he joined the Faculty of Engineering, University of Technology Sydney, as a Lecturer. In 2006, he joined The Hong Kong Polytechnic University, where he spent about six years in the teaching of electronic and information engineering. In 2012, he joined the Institute for Infrastructure Engineering, University of Western Sydney, as a Research Fellow. In 2015, he joined the Qingdao University of Technology (QUT), China, as a Cross-Disciplinary Research Professor and a Supervisor of Ph.D. students. He is a Core Member of the Taishan Scholar Priority Discipline Talent Group, QUT, where he set up the Civionics Research Laboratory. He has authored or co-authored about 110 publications (SCI and EI) in various areas of electrical and civil engineering. His current research interests include passive wireless sensors for structural health monitoring, cement-based materials design and characterization, microwave antennas, and metasurface designs.

Dr. Chung is a member of International Steering Committee of the IEEE International Workshop on Electromagnetics (iWEM). He was the Vice Chair and the Chairman of the IEEE AP/MTT Hong Kong Joint Chapter, in 2010 and 2011, respectively. He is also the General Chair of the iWEM2019. He has been the Founding Chair of the IEEE Qingdao AP/MTT/COM Joint Chapter, since 2017. He acts as a Reviewer for numerous IEEE, IET, Elsevier, and other international journals. He has been an Associate Editor of the IEEE Access, since 2016.

JIEXIN LAI was born in Zhanjiang, Guangdong, China, in 1993. He received the B.S. degree from Shenzhen University, in 2016, where he is currently pursuing the M.S. degree. His research interests include wideband antenna, indoor antenna, and miniaturized antenna.

QINGSHENG ZENG (S'97–M'02–SM'11) received the Ph.D. degree from the University of Ottawa, Canada. He has been a Research Engineer and a Senior Research Engineer with the Communications Research Centre Canada, Canada. He is currently a Distinguished Professor and a Ph.D. Advisor with the Nanjing University of Aeronautics and Astronautics, an Adjunct Professor and a Ph.D. Advisor with the University of Ottawa, Carleton University, the Université du Québec en Outaouais, and the Institut National de la Recherche Scientifique—Centre Energie and Matériaux et Télécommunications, and a Guest Professor with Harbin Engineering University, Northwestern Polytechnic University, the Beijing University of Post and Telecommunications, and Beijing Jiaotong University. He has published over 100 SCI- and EI-indexed papers and technical reports, authored one book and co-authored two book chapters, one of which has been downloaded over 3000 times only in one year after it was published, in 2011. He has undertaken research and teaching in several fields, including antenna analysis and design, electromagnetic compatibility and interference (EMC/EMI), ultra-wideband technology, radio wave propagation, and computational electromagnetics. He is a member of the IEEE Canada Industry Relations Committee. He has been a member of the Strategic Projects Grant Selection Panel (Information and Communications Technologies B) for the Natural Sciences and Engineering Research Council of Canada (NSERC), a member of the Site Visit Committee of the NSERC Industrial Research Chair, and a Reviewer of the NSERC Industrial Research and Development Fellowships. He is the Chair of the AP/MTT Joint Chapter and the Secretary of the EMC Chapter of the IEEE Ottawa. His work on the project Aggregate Interference Analysis and Suitability of Some Propagation Models to Ultra-Wideband Emissions in Outdoor Environments has formed one part of the Consultation Paper on the Introduction of Wireless Systems Using Ultra Wideband Technology, Spectrum Management and Telecommunications Policy, Industry Canada, and has been taken as a significant contribution to the International Telecommunication Union. He received several technical and technical service awards, was ranked as one of the researchers at the Communications Research Centre Canada with the strongest impacts, in 2011, and selected as a Distinguished Expert under the Plan of Hundreds of Talents of Shanxi Province in China, in 2015, and an Oversea Prestigious Advisor of Guangdong Province, in 2017. He has been serving as an Editorial Board Member and a Reviewer for a number of technical books and scientific journals and the Conference Co-Chair, the Session Chair, an Organizer, the Technical Program Committee Co-Chair, a member, a Reviewer, a Short Course/Workshop/Tutorial Presenter, and a Keynote Speaker for many international and national symposia.